International Journal of Environmental Science and Technology
https://doi.org/10.1007/s13762-022-04135-6

ORIGINAL PAPER

Volatile organic compounds constituents of a typical integrated iron and steel plant and influence on O_3 pollution

Y. Wang[1] · R. Zhu[1] · X. Bo[2] · M. Dan[3] · M. Shu[3]

Received: 9 April 2021 / Revised: 30 November 2021 / Accepted: 19 March 2022
© The Author(s) under exclusive licence to Iranian Society of Environmentalists (IRSEN) and Science and Research Branch, Islamic Azad University 2022

Abstract

A typical integrated iron and steel plant in the Beijing–Tianjin–Hebei (BTH) of China was selected to measure volatile organic compound (VOC) constituents from five exhaust stacks belonging to the air heaters, coking, converters, heads, and tails of the sintering machines. The VOC source profiles were established based on the process, and the contribution of VOCs to ozone formation was analyzed in combination with the ozone formation potential (OFP). The concentration of total VOCs (TVOCs) emitted by different processes in the steel plant was 140.5–364.2 μg/m^3. The sequence of TVOC concentrations was as follows: sinter-tail > coking ≈ sinter-head > converter > air heater. Alkanes and aromatic compounds were the predominant groups constituting 48.3% and 36.6% of the VOC concentration, respectively. However, the calculated results with OFP were different, and the contribution of aromatics reached a maximum of 59.8%, followed by alkanes (30.7%). The sequence of OFP for different processes was sinter-head > sinter-tail > coking > converter > air heater. The sinter-head became the segment that contributed the most to ozone formation in the plant; the reason was that the exhaust from sinter-head contained a large amount of aromatic species, which tend to have a greater maximum incremental reactivity (MIR) due to the difference in chemical reactivity.

Keywords Volatile organic compounds · Steel industry · Source profiles · Ozone formation potential

Introduction

In recent years, with the implementation of various emission reduction measures, the emissions of sulfur dioxide (SO_2), nitrogen oxides (NO_x), and particulate matter (PM) from various pollution sources in China have been effectively reduced (Tang et al. 2019). The $PM_{2.5}$ level in the ambient air has also decreased. However, the concentration of ozone (O_3) in the air has increased (Li et al. 2019; Wang et al. 2019).

VOCs are major air pollutants and play an important role in ozone formation (Carter 1994; Han et al. 2018; Lewis et al. 2020). In the atmosphere, they can chemically react with NO_x and hydroxyl (OH) radicals under sunlight to form ground-level ozone and even take part in the formation of haze (Atkinson and Arey 2003; Chen et al. 2020; Ehn et al. 2014), which is the most serious air pollution that has plagued the Beijing–Tianjin–Hebei region in China for a long time (Duan et al. 2008; Huang et al. 2014). More importantly, some VOC species, including benzene and trichloroethylene, are carcinogenic and toxic, may cause irritation to the eyes and skin, and may be harmful to the bronchus (Xiong et al. 2020).

Industrial production and the combustion of fossil fuels are considered the main anthropogenic sources of VOCs in the atmosphere (Jia et al. 2018; Ribeiro et al. 2012). Coke ovens and sintering machines used in integrated iron and steel plants are identified as major sources of non-methane

Editorial responsibility: Rangabhashiyam S.

✉ X. Bo
boxin@buct.edu.cn

[1] School of Environmental Science and Engineering, Tianjin University, Tianjin 300354, People's Republic of China

[2] Department of Environmental Science and Engineering, Beijing University of Chemical Technology, Beijing 100029, People's Republic of China

[3] Institute of Urban Safety and Environmental Science, Beijing Academy of Science and Technology, Beijing 100054, People's Republic of China

Published online: 19 April 2022

VOCs in Europe (Lagoudi et al. 2001). The iron and steel industry is a typical resource and energy-intensive industry, using a series of closely linked processes, including coking, sintering, ironmaking, steelmaking, casting, and rolling. These processes include complex reactions such as pulverization and combustion of raw ore, fuel combustion, and high-temperature smelting (Long et al. 2016), which results in the emission of large amounts of pollutants, especially air pollutants including PM, SO_2, NO_x, and VOCs. VOC mainly came from sintering, coking, air heaters, and converters (Salameh et al. 2016; Wu et al. 2015). It was reported that the VOCs emission characteristics of iron and steel plants are related to their processes (Jiun-Horng et al. 2008).

At present, research on the source profiles of VOCs in different emission resources has become an important issue. Several studies have reported VOC emissions from biomass burning (Jumpponen et al. 2013), various vehicles (Yao et al. 2015a, 2015b), solvent production and usage (Niu et al. 2021; Zhang et al. 2020), refineries (Xiong et al. 2020), and the pharmaceutical chemical synthesis industry (Cheng et al. 2021). Furthermore, several studies have attempted to discuss the profile characteristics of VOCs from the iron and steel industries. Jiun-Horng et al. (2008) reported that 68 VOCs were measured from an integrated iron and steel plant located in Taiwan, including coking, sintering, hot forming, and cold forming processes. The results showed that toluene, 1,2,4-trimethylbenzene, and isopentane were the predominant VOC species. Ciaparra et al. (2009) reported that benzene was the VOC species with the predominant concentrations in two integrated steelworks in the UK. Shi et al. (2015) studied 107 kinds of VOC mass concentrations and profiles for iron smelt and coke production plants in Liaoning Province and found that halogenated hydrocarbons exhibited higher mass percentages for the VOC source profiles. Zhang et al. (2020) monitored VOCs emissions from a typical iron and steel plant in Yangtze River Delta (YRD); the results indicated that benzene, ethene, ethane, toluene, and *m,p*-xylene aromatics were the predominant precursors. Obviously, there were certain variations across these VOC source profiles in different regions. In another words, the representativeness of existing source profiles was not comprehensive and might result in large uncertainty in the source apportionment of VOCs, thus further misleading the policy made for air pollution control. Therefore, VOC source profiles need to be constantly enriched and developed.

The Beijing–Tianjin–Hebei region is home to the largest number of large-scale iron and steel plants in China and the world. Steel plants in the region not only enjoy technological and scale advantages in production but also face more stringent air pollutant emission restrictions. In order to ensure the accuracy of emission inventories and source contributions, a comprehensive and real-time updated VOCs profile about a typical integrated iron and steel plant is called for creation in this region. The objectives of this study were to conduct organized exhaust sampling based on production processes to identify and compare the emission characteristics of various processes in the steel industry. For the first time, the concentration, emission characteristics, and ozone formation potential (OFP) of VOCs were measured to create a profile from various processes in an integrated iron and steel plant in the BTH, which is of great importance for the government to refine the management of the steel industry and the selection of key VOC species under the control of the industry.

Materials and methods

Sampling sites and date

The integrated iron and steel plant, located in Cangzhou, Hebei Province, China, was established in 2006. Its annual output exceeds 10 million tons, and its products are mainly iron and steel products such as train car plates and container plates. The company is the largest long-process steel plant in Cangzhou, including sintering, pelletizing, coking, blast furnace, converter, cold rolling, and other auxiliary processes.

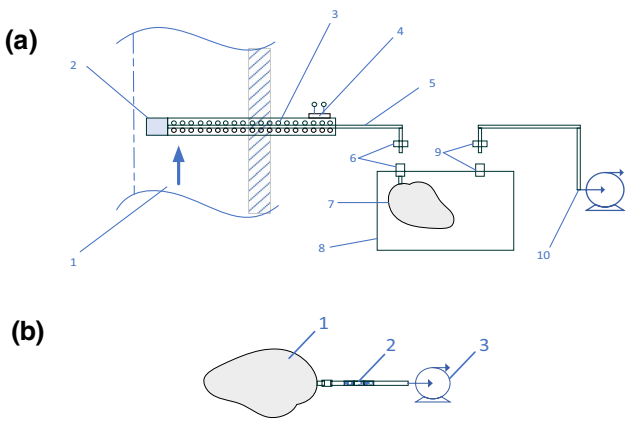


Fig. 1 **a** Schematic diagram for connection of the sampling line: (1) exhaust flue; (2) filter head; (3) sampling catheter; (4) heaters; (5) sampler; (6) sampling box inlet and valve; (7) Teflon gas sampling bag; (8) vacuum gas sampling box; (9) sampling box outlet and valve; (10) pump. **b** Schematic diagram for the enrichment of the sampling line: (1) gas collection bag; (2) adsorption tube; (3) sampler

The important plants include converters, air heaters, sintering machines, and coke-making equipment to produce cast steel. The sampling took place on September 15, 2020.

Sample collection

Organized exhaust sampling was carried out with reference to *HJ732-2014 Air Bag Method for Sampling of Fixed Pollution Source Waste Gas and Volatile Organic Compounds*" (Ministry of Ecology and Environment of the People's Republic of China. 2014a). The specific sampling scheme is shown in Fig. 1. Exhaust gases discharged through the stack of a stationary source are collected and saved directly into Teflon gas bags using equipment such as vacuum boxes and suction pumps. If the exhaust gas temperature in the stack is higher than the ambient temperature, the sampling tube is preheated to 120 °C and then sampled. The pump was connected to the sampling gun and turned on, the flow rate was adjusted to 1.0 L/min, and it pumped for approximately 3 min to replace the gas in the sampling tube with the gas in the flue and saturate it with as much adsorption as possible. The pump was turned off when the sampling volume in the airbag reached approximately 80% of the maximum volume of the airbag, and the operation was repeated three times. Immediately after sampling, the gas bag samples were transferred to the adsorption tubes and stored in a volume of 1.0 L. The samples were sealed with sealing caps at both ends of the adsorption tubes immediately after transfer, wrapped in aluminum foil, and stored in sealed bags, protected from light, and dried at 4 °C. The analysis was completed within one week.

In order to ensure the accuracy of sampling, the plant was in full production during the sampling process. The samples include four air heater stack exhaust samples, four coking stack exhaust samples, four sinter-head samples, four sinter-tail samples, and two secondary fumes from the converter samples in the process of the iron and steel plant. The specific sampling information, operating conditions, and baseline information of the exhausts are listed in Table 1.

Sample analysis

This analysis followed the national standard *HJ734* (Ministry of Ecology and Environment of the People's Republic of China. 2013) and *HJ644 methods* (Ministry of Ecology and Environment of the People's Republic of China. 2014b), using a QP2010 gas chromatography–mass spectrometry (GC–MS) to test 56 VOCs shown in Table 2. The adsorption tube was aged first, at a temperature of 350 °C with a flow rate of 40 mL/min for 15 min. Then, the sample was concentrated by cold hydrazine, the temperature of the transfer line was 150 °C, the initial temperature of the adsorption tube was 20 °C, the initial temperature of cold hydrazine was − 10 °C, the concentration after the sample was subjected to thermal analysis, the adsorption tube desorption temperature was 320 °C, the adsorption tube desorption time was 10 min, the cold hydrazine desorption temperature was 310 °C, the cold hydrazine desorption time was 5 min, the dry blowing flow was 30 mL/min, the dry flowing time was 2 min, and the split flow rate was 15 mL/min. After thermal desorption, the sample entered the gas chromatographic separation and was detected by a mass detector, and the results were qualitatively compared with the mass spectrum and retention time of the standard substance. Chromatographic conditions: chromatographic column DB-624 30 m × 0.25 mm × 1.40 μm; carrier gas: helium; column flow: 1.2 mL/min; heating program: initial temperature 35 °C, for 6 min and heating of 5 °C/min to 230 °C, hold for 5 min; mass spectrometry conditions: full scan; scanning range: 35–370 amu; ionization energy: 70 eV; ion source temperature: 220 °C; transmission line temperature: 200 °C.

In total, 56 individual VOC species were analyzed in this study, including 5 alkanes, 2 olefins, 12 aromatics, 26 halogenated hydrocarbons, and 11 oxygenated VOC (OVOC) species, as shown in Table 2.

Table 1 Sampling information, operating conditions, and baseline information of exhaust from the various processes in the steel plant

Processes	Sampling sites	Fuel types	Temperature (°C)	Gas flow rate ($Nm^{3(a)}/h$)	O_2 (%)	H_2O (%)
Air heater	Stack	Coke	93–116	48,605–49,231	5.6–8.2	4.3–5.5
Coking	Stack	BFG[b]/COG[c]	85–88	325,102–325,203	8.9–0.7	8.4–9.7
Sinter-head	Stack	COG	75–83	309,806–309,925	13.2–15.9	6.8–7.5
Sinter-tail	Stack	COG	112–124	192,231–192,345	12.9–15.4	6.5–7.6
Converter	Stack	–	85–105	203,818–254,038	14.3–18.8	4.5–5.8

[a]Gas condition at 1 atm and 0 °C

[b]Blast furnace gas

[c]Coke oven gas

Table 2 The 56 analyzed VOC components

No	Groups	Components	No	Groups	Components
1	Alkanes	*n*-Hexane	30	Halogenated	1,2-Dichloroethane
2		*n*-Heptane	31		Trichloroethylene
3		*n*-Decane	32		1,2-Dichloropropane
4		*n*-Undecane	33		Cis 1,3-dichloropropene
5		*n*-Dodecane	34		1,3-Dichloropropene
6	Olefin	1-Decene	35		1,1,2-Trichloroethane
7		1-Dodecene	36		Perchloroethylene
8	Aromatics	Benzene	37		1,2-Dibromoethane
9		Toluene	38		Chlorobenzene
10		Ethylbenzene	39		1,1,2,2-Tetrachloroethane
11, 12		*m,p*-xylene	40		1,3-Benzene
13		Styrene	41		1,4-Dichlorobenzene
14		*O*-xylene	42		Benzyl chloride
15		*n*-Propylbenzene	43		1,2-Dichlorobenzene
16		4-Ethyltoluene	44		1,2,4-Trichlorobenzene
17		1,3,5-Trimethylbenzene	45		Hexachlorobutadiene
18		1,2,4-Trimethylbenzene	46	Oxygenated	Acetone
19		1,2,3-Trimethylbenzene	47		Acetone
20	Halogenated	Methyl bromide	48		Ethyl acetate
21		1,1-Dichloroethylene	49		Hexamethyldisiloxane
22		1,1,2-Trichloro-1,2,2-trifluoroethane	50		3-Pentanone
23		Chloropropylene	51		Cyclopentanone
24		Dichloromethane	52		Butyl acetate
25		1,1-Dichloroethane	53		PGEA
26		Cis 1,2-dichloroethylene	54		2-Heptanone
27		Trichloromethane	55		Benzaldehyde
28		1,1,1-Trichloroethane	56		Anisole
29		Carbon tetrachloride			

The emission source composition spectrum can also be called the *"source fingerprint"*, as there is no standard definition. It generally refers to the relative chemical components in the complex pollutants (such as $PM_{2.5}$ and VOCs) emitted by various air pollution sources. The proportion of total pollutant emissions is expressed as a mass percentage. The composition spectrum of the emission sources is the statistical average of emissions from similar emission sources. Important information to quantify the characteristics of emission sources is the most basic data for source analysis.

This study followed the *"Average source spectrum construction method,"* that is, the exhaust of each process unit is calculated via the direct average concentration (Lorenzi et al. 2015). In the present study, the percentage of individual VOC component in the average source spectrum was calculated using Eq. (1):

$$X_i = \frac{\sum_{j=1}^{n} x_{ij}}{n} \quad (1)$$

where i is the VOC component, j is the production process, X_i is the percentage of component i in the average source spectrum, and n is the number of production processes.

Ozone formation potential

VOCs play a vital role in the formation of photochemical smog. The OFP is a well-known and commonly used parameter to describe the impact of individual VOC on O_3 production (Li et al. 2019; Song et al. 2018) The MIR scale is also the most commonly used version of the control strategy across the USA, as it applies to urban environments with high NOx, in such environment, VOC controlling is an

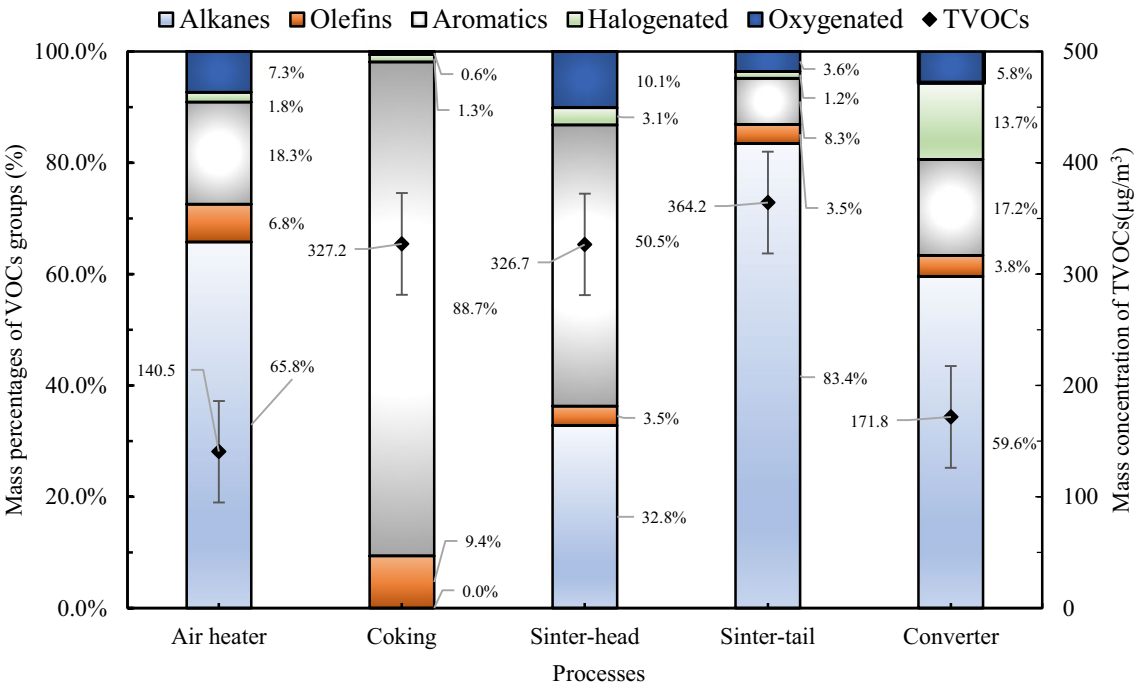


Fig. 2 Concentration of TVOCs and mass percentages of VOC groups based on production processes

effective strategy to reduce ozone (Venecek et al. 2018). In order to evaluate the impact of the VOC species on ozone formation, the ozone formation potentials (OFP) of each VOC species was calculated by multiplying the emissions by its corresponding maximum increment reactivity (MIR) factor (Carter and Atkinson 1987; Carter 1994; Russell et al. 1995). In the present study, the OFP of individual VOCs was calculated using Eq. 2:

$$OFP_i = MIR_i \times VOC_i \tag{2}$$

where OFP_i (μg/m^3) refers to the ozone generation potential of component *i*; VOC_i (μg/m^3) represents the mass concentration of the *i* VOC; MIR_i (O_3 g/VOC g) is the maximum incremental reactivity scale for species *i*. The development of the MIR scale for individual VOCs was originally proposed by (Carter 1994) based on the SAPRC-07 mechanism and was recently updated by Venecek et al. (2018). The species without MIR values were ignored in the calculation of OFP, it ought to be noted.

Results and discussion

Mass concentration and group weight

As shown in Fig. 2, the concentrations of TVOCs emitted by different production processes in the steel plant were 140.5–364.2 μg/m^3. Due to limitation of space, the concentration of each VOC species in various processes is shown in appendix. The sequence of contribution for TVOCs emitted by the stack was as follows: sinter-tail (27.4%) > coking (24.6%) ≈ sinter-head (24.6%) > converter (12.9%) > air heater (10.6%). The concentration of sinter-tail was approximately 2.5 and 2.1 times that of the air heater and secondary fumes of the converter. The large amount of VOCs from the sinter-head was mainly from the combustion of iron ore and anthracite coal. Although the TVOC concentrations at the sinter-head and sinter-tail were much lower than those of typical steel plants in Sichuan (Liu et al. 2020) and Liaoning (Shi et al. 2015) provinces, the sintering process was the process with the highest concentration of TVOCs.

From the structural characteristics of the different species of organized emissions of VOCs from steel plants, it can be observed that the composition of VOCs emitted from different processes has a very different ratio. Alkanes were the major VOCs measured by mass percentage, accounting for 45.0% of the total VOCs, followed by aromatics (41.5%). The concentrations of olefins, oxygenated, and halogenated VOCs were relatively low, accounting for 3.4–5.5% of the total VOCs. These results were not consistent with some previous studies (Jiun-Horng et al. 2008; Liu et al. 2020; Zhang et al. 2020), which showed that aromatics were the dominant VOCs species in iron and steel plant.

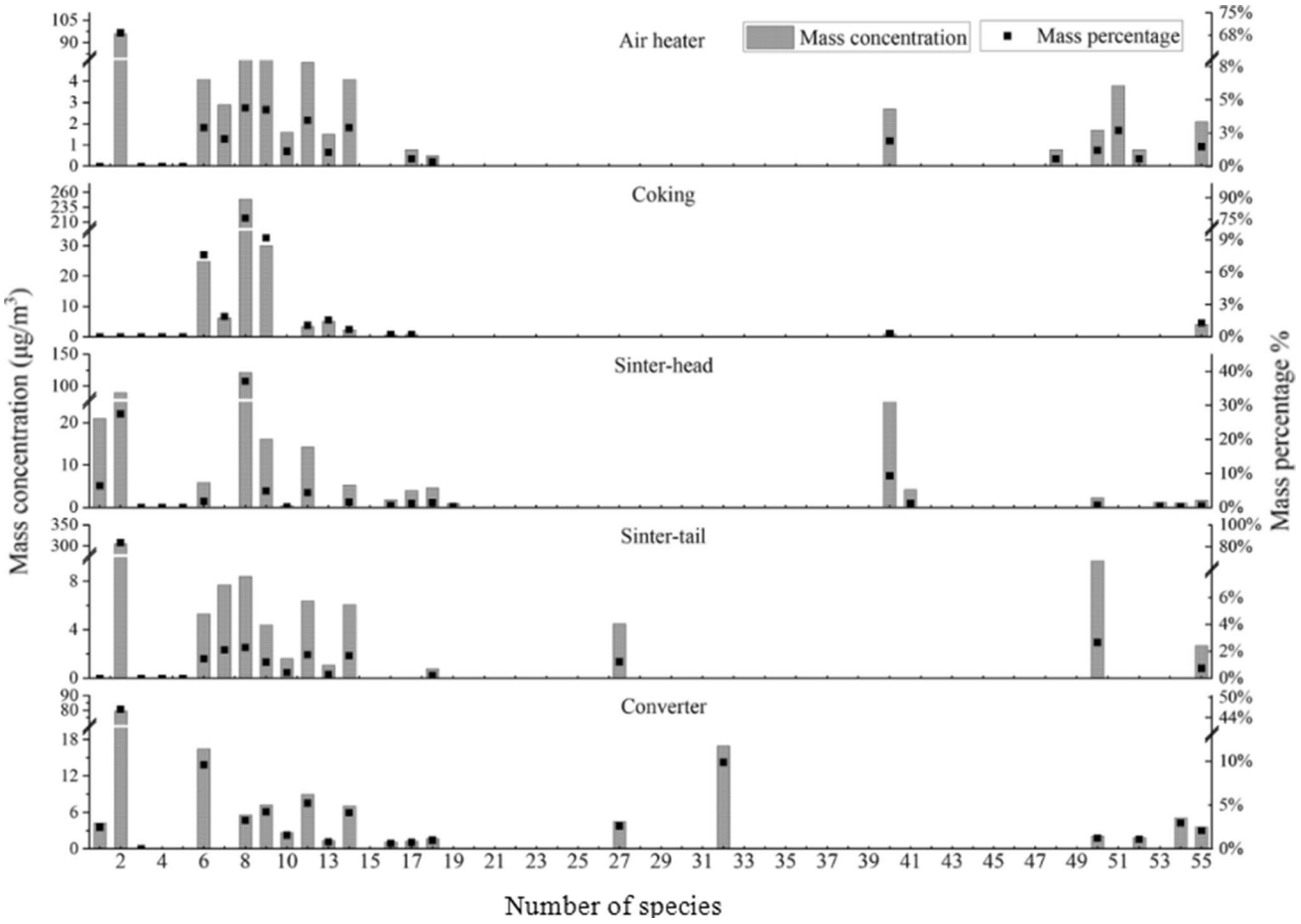


Fig. 3 VOC source profiles of various processes in steel plant

In terms of the total emissions of VOCs, the concentration detected by different studies varied greatly. Taking the coking process, which has been widely reported in previous studies, as an example, 56 VOC species from cooking process were detected in this study, and the total mass concentrations were 327.23 μg/m^3; however, 107 VOC species from an iron and steel plant in Liaoning Province were concerned in Shi et al.'s (2015) study, with the total mass concentrations of 10,918 μg/m^3, and 86 VOC species from an iron and steel plant in Sichuan Province (Liu et al 2020) were studied, with the total mass concentrations were 1030.74 μg/m^3.

Source profiles

Figure 3 shows the mass concentration and mass percentage of VOC species based on various production processes in the steel plant. The major VOC species in the air heater process included *n*-heptane, benzene, toluene, 1-dodecene, *m,p*-xylene, 1-decene, *o*-xylene, cyclopentanone, and 1,3-dichlorobenzene; their concentrations varied from 2.1 to 96.0 μg/m^3. The mass percentage of alkanes in this process stood out because of the high concentration of *n*-hexane (96.0 μg/m^3), with a mass percentage of 65.8%. The detectable aromatic compounds included benzene, toluene, *m,p*-xylene, and *o*-xylene; their concentrations were 4.1–6.2 μg/m^3. Olefinic species, such as 1-decene and 1-dodecene, were detected at concentrations of 4.1 μg/m^3 and 2.9 μg/m^3, respectively. The concentrations of the oxygenated VOCs 3-pentanone cyclopentanone and 1,3-dichlorobenzene were 1.7–3.8 μg/m^3. The steel plant in the present study had two air heaters, both using blast furnace gas as fuel; because the composition of blast furnace gas is more complex, there are more species in the air heater stack. Halogenated species and oxygenated VOCs (OVOCs) were also detected, and their mass percentages were low (< 5%).

The major VOC species in the coking process included benzene, toluene, 1-decene, 1-dodecene, styrene, benzaldehyde, *p*-xylene, and *o*-xylene, which accounted for 97.9% of the total mass percentage in the process, most of them were aromatic compounds. Benzene, toluene, and 1-decene were the three components with the highest concentrations at 248.5 μg/m^3 (75.5%), 30.0 μg/m^3 (9.1%), and 24.8 μg/m^3 (7.5%), respectively. In general, coking is a reducing condition, and coking coal is aromatic, which results in a large number of aromatic compounds in the coking gas (Jiun-Horng et al. 2008). Some olefinic species, including 1-decene and 1-dodecene, were detected, with concentrations of 24.9 μg/m^3 and 6.2 μg/m^3, respectively. The other three species were not detected in the coking process.

At the head of the sintering machine, the major VOC species in the exhaust included benzene, *n*-heptane, 1,3-dichlorobenzene, *n*-hexane, toluene, *p*-xylene, 1-decene, *o*-xylene, and 1,2,4-trimethylbenzene. The concentrations of these VOC species ranged from 4.7 to 121.0 μg/m^3, and their mass percentages cumulatively accounted for 92.9% of this process. The exhaust from the head of the sintering machine is mainly generated by the burning of sintering raw materials (iron ore, quicklime, etc.) and fuel (anthracite), which has a higher concentration and contains more species of pollutants. Most were aromatics and alkanes; the detected aromatics included benzene, toluene, *o*-xylene, and *m/p*-xylene; the concentration of benzene was 121.1 μg/m^3, and the others were 5.3 to −16.1 μg/m^3. The detected alkanes were *n*-hexane and *n*-heptane, with concentrations of 21 μg/m^3 and 90 μg/m^3, respectively. The concentrations of detectable halogenated hydrocarbons, including 1,3-benzene, 1,4-dichlorobenzene, and 3-pentanone, ranged from 2.3 to 30.3 μg/m^3.

The major VOC species at the tail of the sintering machine included *n*-heptane, 3-pentanone, benzene, 1-dodecene, *p/m*-xylene, *o*-xylene, 1-decene, toluene, and chloroform; these components accounted for 98.3% of the total VOCs. The concentrations of major VOC species were between 4.4 and 301.0 μg/m^3. The pollutants at the tail of the sintering machine mainly come from the unloading and the dust-containing gas released during the crushing, screening, storage, and transportation of the adjacent sintered ore. *n*-Heptane was the only alkane species detected in the exhaust emitted by the tail exit of the sintering machine, but the concentration was as high as 305.5 μg/m^3 (83.9%). Benzene, *p/m*-xylene, *o*-xylene, and toluene were classified as aromatic species, and their concentrations ranged from 4.4 to 8.4 μg/m^3. The detectable OVOCs, including 3-pentanone and benzaldehyde, and olefinic species, such as 1-decene and 1-dodecene, had concentrations of less than 10 μg/m^3.

In the converter process, the major VOC species included *n*-heptane, 1,2-dichloropropane, *p*-xylene, *o*-xylene, 1-decene, toluene, 3-pentanone, benzaldehyde, and benzene, with concentrations from 5.0 to 179.4 μg/m^3. The secondary fumes of the converter mainly come from the exhaust emitted by the sputtering of the steel when the converter is blended with the iron, which has a high concentration of fumes. The detectable alkanes species included *n*-heptane and *n*-hexane; the concentration of the former was 79.6 μg/m^3 (46.3%) and that of the latter was 4.3 μg/m^3. A special component was detected only in the secondary fume gas of the converter at a concentration of 17 μg/m^3. The concentrations of aromatics and OVOCs were less than 8 μg/m^3.

Similar to the previous discussion, source profiles of VOCs in this study were compared with two plants in Liaoning (Shi et al. 2015) and Sichuan (Liu et al. 2020). Benzene, toluene, and *m/p*-xylene were all detected in cooking and sinter-tail segments in three studies; for other VOCs species, there were significant differences among the three studies. It was worth mentioning that *n*-heptane occupied the first mass percentage in the sintering process in the study, while benzene had the largest mass percentage in Shi et al.'s (2015) study, and in Liu et al.'s (2020) study the largest one was carbon disulfide. The reason for the differences may be related to the different performance for cleaner production and composition characteristics of coal feedstock in different regions. For instances, in Liu et al.'s (2020) study and this study, both steel plants were equipped with exhaust gas treatment equipment, but it was not mentioned in Shi et al.'s (2015) study.

Ozone formation potential of VOCs

Ozone formation potential (OFP) is a common parameter to show the impact of individual VOC on O_3 production. The higher OFP means the higher contribution of VOC transforming to O_3. The OFP for each specie in the study was calculated based on the mass concentration of each specie, and corresponding MIR is shown in Table 3. The concentrations of OFP for various processes in the steel plant were 247.7–558.8 μg/m^3, which were significantly smaller than the 760.08–2391.90 μg/m^3 for typical steel plant in the YRD (Zhang et al. 2020) and the 94,811–408,142 μg/m^3 for an integrated iron and steel plant in Taiwan (Jiun-Horng et al. 2008). The total OFP value of 2092.28 μg/m^3 in the present was also significantly smaller than that of other existing studies. The results indicated that the potential for ozone formation from VOCs in the processes of this steel plant in

Table 3 Ozone formation potential (μg/m^3) of major VOC species in the exhaust of various processes

NO	Groups		MIR[a] O_3 g/VOC g	Air heater	Coking	Sinter-head	Sinter-tail	Converter	Total
1	Alkanes	*n*-Hexane	1.240	0.00	0.00	26.04	0.00	5.33	31.37
2		*n*-Heptane	1.070	102.72	0.00	96.30	326.89	85.17	611.08
6	Olefins	1-Decene	2.170	8.90	54.03	12.80	11.50	35.81	123.04
7		1-Dodecene	1.640	4.76	10.17	0.00	12.63	0.00	27.55
8	Aromatics	Benzene	0.720	4.46	178.92	87.19	6.05	4.03	280.66
9		Toluene	4.000	24.00	120.40	64.40	17.60	29.20	255.60
10		Ethylbenzene	3.040	4.86	0.00	1.52	4.86	8.21	19.46
11,12		*m/p*-xylene	8.700	42.63	30.45	124.41	55.68	78.30	331.47
13		Styrene	1.730	2.60	8.82	0.00	1.90	2.42	15.74
14		*O*-xylene	7.640	31.32	16.81	40.49	46.60	54.24	189.47
17		1,3,5-Trimethylbenzene	11.760	9.41	9.41	47.04	0.00	15.29	81.14
18		1,2,4-Trimethylbenzene	8.870	4.44	0.00	41.69	7.10	15.08	68.30
19		1,2,3-Trimethylbenzene	11.970	0.00	0.00	10.77	0.00	0.00	10.77
32	Halogenated	1,2-Dichloropropane	0.280	0.00	0.00	0.00	0.00	4.76	4.76
41		1,4-Dichlorobenzene	0.171	0.00	0.00	0.72	0.00	0.00	0.72
48	OVOCs	Ethyl acetate	0.590	0.47	0.00	0.00	0.00	0.00	0.47
50		3-Pentanone	1.240	2.11	0.00	2.85	12.03	2.60	19.59
51		Cyclopentanone	1.150	4.37	0.00	0.00	0.00	0.00	4.37
52		Butylacetate	0.770	0.62	0.00	0.00	0.00	1.46	2.08
54		2-Heptanone	2.360	0.00	0.00	2.60	0.00	12.04	14.63
		Total		247.66	429.01	558.83	502.84	353.95	2092.28

(a) MIR denotes the maximum incremental reactivity of a specific compound, as cited from Venecek et al. (2018) and Xiong et al. (2020)

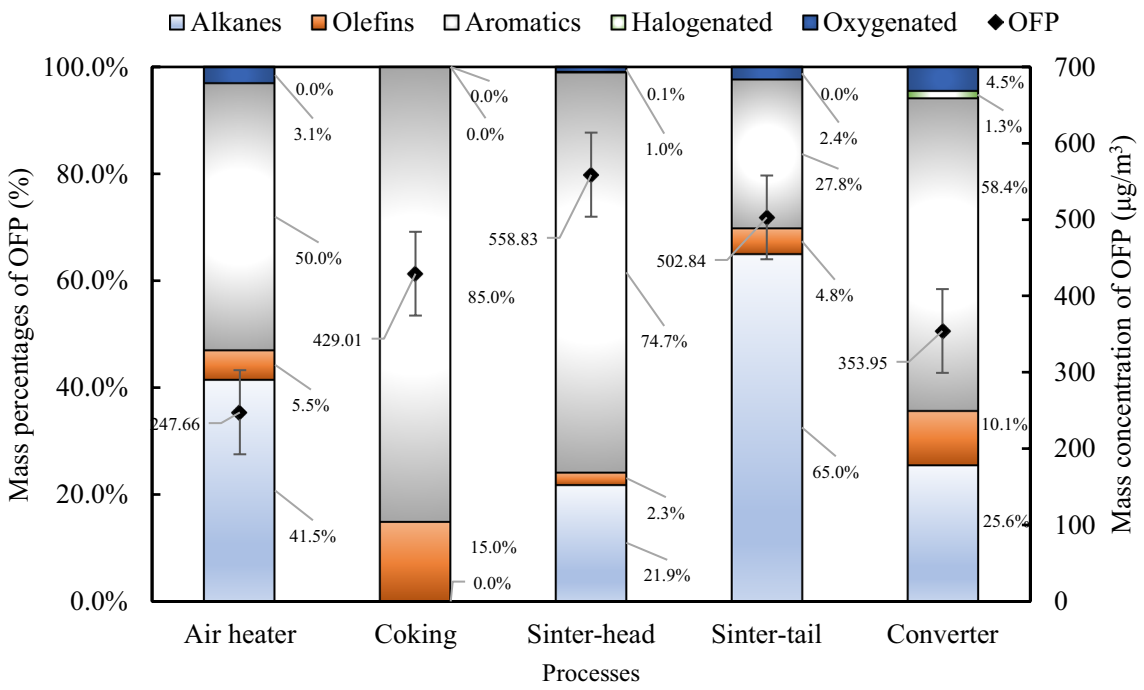


Fig. 4 Ozone formation potential (OFP) and mass percentages of VOC groups based on production processes

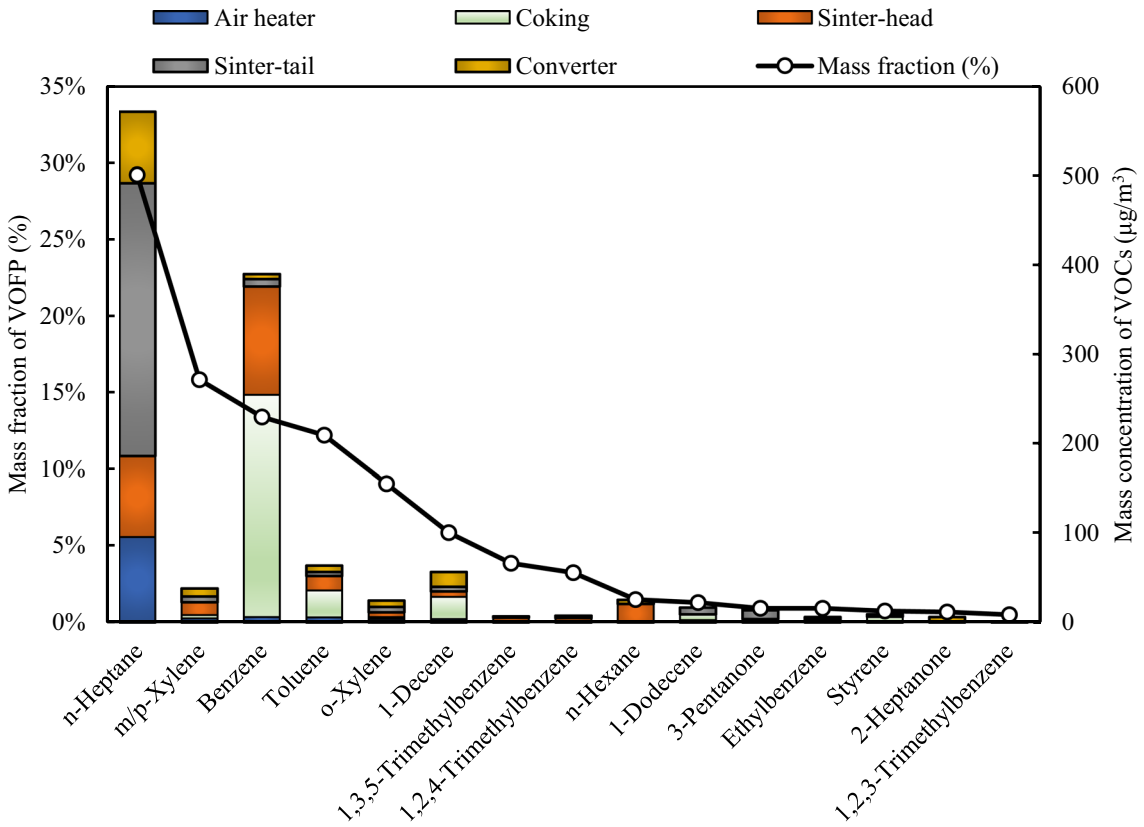


Fig. 5 Comparison of OFP of major VOCs emitted by various processes

BTH was significantly smaller than that of existing studies in other regions of China. It can be ascribed to the decrease of the concentration of each individual VOC, especially for the species with large MIR such as toluene, *m/p*-xylene and trimethylbenzene, which correspondingly results in the sharp reduction of the OFPs. Such reduction demonstrated the effectivity of VOC emission control strategy in the steel plant.

Figure 4 shows the sequence of OFP for various processes: sinter-head (26.7%) > sinter-tail (24.0%) > coking (20.5%) > converter (16.9%) > air heater (11.8%). The OFP of the sinter-head and sinter-tail exhaust was approximately 1.6 and 2.3 times that of the secondary fume of the converter and air heater, respectively. This ranking differed from the former ranking of TVOC concentration; although the concentration of TVOCs at the head of the sinter was lower than those in the sinter-tail and coking processes, the sinter-head became the process with the highest OFP; the reason was that the exhaust contained more species with larger maximum incremental reaction activity, such as toluene, *m/p*-xylene, 1,3,5-trimethylbenzene, and 1,2,4-trimethylbenzene. The OFP sequence of the VOC group was as follows: aromatics (59.9%) > alkanes (30.7%) > olefins (7.2%) > oxygenated (2.0%) > halogenated (0.3%). Aromatics were the main contributors of OFPs instead of alkanes. These results were in accordance with previous studies reporting a disproportionate relationship between VOC level and associated OFP (Song et al. 2018; Wu et al. 2017; Zheng et al. 2018). From the perspective of chemical reaction mechanism, VOC is a potential contribution to the formation of ozone, and the main chemical reactions are a series of complex reactions between VOCs and OH radicals, nitrate (NO_3) radicals and O_3. According to Atkinson's study (2003), the reaction rate constants of different VOCs with OH radicals, NO_3 radicals and O_3 are different, and the order of reaction rate constants with OH radicals is: alkane < alkene < aromatic, the order of reaction rate constant with O_3 is as follows: olefin < aromatic, and the order of reaction rate constants with NO_3 radicals is: alkane < alkene < aromatic. Therefore, it can be found

that the reaction rate of different types of VOC is different, which is also reflected in their MIR value. The MIRs of aromatic hydrocarbon and olefin are generally larger than that of alkanes, and aromatic VOCs has a reaction advantage in the formation of ozone.

Table 3 lists the OFP for individual VOC species, and Fig. 5 lists the top 15 individual VOC species that contributed the most to the OFP. *n*-Heptane was the most significant contributor to O_3 formation in the steel plant, accounting for 29.2% of the total OFP, followed by *m/p*-xylene (15.8%), benzene (13.4%), toluene (12.2%), *o*-xylene (9.1%), and 1-decene (5.9%). The contribution of *n*-heptane to OFP in plant was relatively higher than that observed in YRD region (6.3%) (Zhang et al. 2020), and Taiwan (4.2%) (Jiun-Horng et al. 2008), highlighting the importance of reducing *n*-heptane emission in the steel plant based on its O_3 formation potential.

The OFP of the species exhausted by different processes were divided by the total OFP to obtain the proportion of each species' contribution to the OFP, and the proportions were added. As shown in Fig. 5, almost all aromatic VOCs occurred in the coking process (53.1%) and the sinter-head (31.6%). Conversely, the sources of *n*-heptane were diverse; other processes were involved, except for coking. The sintering process exhausted the largest amount of *n*-heptane, and the tail of the sintering machine contributed 53.5% of it. Furthermore, 54.3% of the species *m/p*-xylene that contributed a lot to OFP came from the sintering process, and 23.6% came from the secondary fumes of the converter.

In summary, the multiple aromatic species in the exhaust contributed the most to ozone formation, followed by *n*-heptane in alkanes; sintering had the greatest environmental impact in the steel production, followed by the coking process. Therefore, under the limited control conditions, it was recommended that the VOCs from the sintering process should be effectively treated, including sinter-head and sinter-tail, which contributed to the reduction of VOC concentration and greatly reduced the potential for ozone formation. In addition, it was possible to further carry out effective collection and treatment of processes such as coking and converter processes with relatively high OFP.

Conclusion

This study constructed a VOC source profile based on the production process of a typical steel plant in the Beijing–Tianjin–Hebei region of China. The results showed that *n*-heptane, benzene, toluene, 1-decene, *m,p*-xylene, 1,3-dichlorobenzene, *n*-hexane, and *o*-xylene were the predominant VOC species in the five processes. N-heptane and benzene were the most dominant species, with a total mass percentage > 70%. Alkanes and aromatic groups were the major groups, constituting 48.3% and 36.6% of the VOC concentrations, respectively.

n-Heptane, *m/p*-xylene, benzene, toluene, *o*-xylene, and 1-decene were the major ozone formation species. Aromatic compounds were the predominant VOC groups, contributing nearly 60% to the OFP in the exhaust emitted by various processes. The sequence of VOC concentrations emitted by the stack was as follows: sinter-tail (27.4%) > coking (24.6%) ≈ sinter-head (24.6%) > converter (12.9%) > air heater (10.6%). However, the sequence of VOC OFP of various processes was as follows: sinter-head (26.7%) > sinter-tail (24.0%) > coking (20.5%) > converter (16.9%) > air heater (11.8%). Nearly 50% of the VOCs and OFP were emitted by the exhaust of the sintering process, which is the production process that requires priority treatment plants for VOCs, including the sintering head and tail.

The aromatic hydrocarbon species emitted from the head of the sintering machine contributed the most to OFP. The hot exhaust from the sintering head can be used secondarily by introducing it into the sintering material layer and decomposing the VOCs in it at high temperatures, or using end-of-pipe treatment methods such as activated carbon adsorption. This study provided a research paradigm for VOC treatment in large-scale iron and steel enterprises in the Beijing–Tianjin–Hebei region.

Supplementary Information The online version contains supplementary material available at https://doi.org/10.1007/s13762-022-04135-6.

Acknowledgements The authors would like to thank all organizations and specialists that helped to prepare this research.

Authors' contributions Rongjie Zhu wrote the manuscript. Yuan Wang supervised the work. Xin Bo supervised the work. Mo Dan was responsible for sampling and analysis. Mushui Shu was responsible for sampling and analysis.

Funding This work was supported by the National Natural Science Foundation of China (41871211; 72174125; 71974141); Fundamental Research Funds for the Central Universities (buctrc202133).

Availability of data and materials All data generated or analyzed during this study are included in this published article.

Declarations

Conflict of interest The authors declare that they have no competing interests.

Ethics approval and consent to participate This article does not contain any studies with human participants or animals performed by any of the authors.

References

Atkinson R, Arey J (2003) Atmospheric degradation of volatile organic compounds. Chem Rev 103:4605–4638. https://doi.org/10.1021/cr0206420

Carter WP, Atkinson R (1987) An experimental study of incremental hydrocarbon reactivity. Environ Sci Technol 21:670–679. https://doi.org/10.1021/es00161a008

Carter WPL (1994) Development of ozone reactivity scales for volatile organic compounds. Air Waste 44:881–899. https://doi.org/10.1080/1073161X.1994.10467290

Chen S, Wang H, Lu K et al (2020) The trend of surface ozone in Beijing from 2013 to 2019: indications of the persisting strong atmospheric oxidation capacity. Atmos Environ. https://doi.org/10.1016/j.atmosenv.2020.117801

Cheng N, Jing D, Zhang C et al (2021) Process-based VOCs source profiles and contributions to ozone formation and carcinogenic risk in a typical chemical synthesis pharmaceutical industry in China. Sci Total Environ 752:141899–141899. https://doi.org/10.1016/j.scitotenv.2020.141899

China MoEaEotPsRo (2013) Ambient air Determination of volatile organic compounds Adsorption tube sampling-thermal desorption/gas chromatography-mass spectrometry vol (HJ 644-2013). China Environmental Science Press, Beijing

China MoEaEotPsRo (2014a) Emission from stationary sources-Sampling of volatile organic compounds-Bags method vol (HJ 732–2014a) China Environmental Science Press, Beijing

China MoEaEotPsRo (2014b) Stationary source emission -Determination of volatile organic compounds-Sorbent adsorption and thermal desorption gas chromatography mass spectrometry method vol (HJ 734—2014). China Environmental Science Press, Beijing

Ciaparra D, Aries E, Booth M-J et al (2009) Characterisation of volatile organic compounds and polycyclic aromatic hydrocarbons in the ambient air of steelworks. Atmos Environ 43:2070–2079. https://doi.org/10.1016/j.atmosenv.2008.09.078

Duan J, Tan J, Yang L et al (2008) Concentration, sources and ozone formation potential of volatile organic compounds (VOCs) during ozone episode in Beijing. Atmos Res 88:25–35. https://doi.org/10.1016/j.atmosres.2007.09.004

Ehn M, Thornton JA, Kleist E et al (2014) A large source of low-volatility secondary organic aerosol. Nature 506:476. https://doi.org/10.1038/nature13032

Han D, Gao S, Fu Q et al (2018) Do volatile organic compounds (VOCs) emitted from petrochemical industries affect regional PM2.5? Atmos Res 209:123–130. https://doi.org/10.1016/j.atmosres.2018.04.002

Huang R-J, Zhang Y, Bozzetti C et al (2014) High secondary aerosol contribution to particulate pollution during haze events in China. Nature 514:218–222. https://doi.org/10.1038/nature13774

Jia J, Cheng S, Yao S et al (2018) Emission characteristics and chemical components of size-segregated particulate matter in iron and steel industry. Atmos Environ 182:115–127. https://doi.org/10.1016/j.atmosenv.2018.03.051

Jiun-Horng T, Kuo-Hsiung L, Chih-Yu C et al (2008) Volatile organic compound constituents from an integrated iron and steel facility. J Hazard Mater 157:569–578. https://doi.org/10.1016/j.jhazmat.2008.01.022

Jumpponen M, Ronkkomaki H, Pasanen P et al (2013) Occupational exposure to gases, polycyclic aromatic hydrocarbons and volatile organic compounds in biomass-fired power plants. Chemosphere 90:1289–1293. https://doi.org/10.1016/j.chemosphere.2012.10.001

Lagoudi A, Lois E, Fragioudakis K et al (2001) Design of an inventory system for the volatile organic compounds, emitted by various activities. Environ Sci Technol 35:1982–1988. https://doi.org/10.1021/es000051w

Lewis AC, Hopkins JR, Carslaw DC et al (2020) An increasing role for solvent emissions and implications for future measurements of volatile organic compounds. Philos Trans R Soc Math Phys Eng Sci. https://doi.org/10.1098/rsta.2019.0328

Li K, Jacob DJ, Liao H et al (2019) Anthropogenic drivers of 2013–2017 trends in summer surface ozone in China. Proc National Acad Sci United States Am 116:422–427. https://doi.org/10.1073/pnas.1812168116

Liu Z, Xu C, Chen J et al (2020) Measurement and composition characteristics of volatile organic compounds emissions from typical steel companies. China Environ Sci 40:4292–4303

Long Y, Pan J, Farooq S et al (2016) A sustainability assessment system for Chinese iron and steel firms. J Clean Prod 125:133–144. https://doi.org/10.1016/j.jclepro.2016.03.030

Lorenzi A, Rastelli D, Biavati A et al (2015) Immobilization of iron rich steel industry waste and products characterization. J Environ Chem Eng 3:196–201. https://doi.org/10.1016/j.jece.2014.11.024

Niu Z, Kong S, Zheng H et al (2021) Temperature dependence of source profiles for volatile organic compounds from typical volatile emission sources. Sci Total Environ. https://doi.org/10.1016/j.scitotenv.2020.141741

Ribeiro J, Silva T, Mendonca Filho JG et al (2012) Polycyclic aromatic hydrocarbons (PAHs) in burning and non-burning coal waste piles. J Hazard Mater 199:105–110. https://doi.org/10.1016/j.jhazmat.2011.10.076

Russell A, Milford J, Bergin MS et al (1995) Urban ozone control and atmospheric reactivity of organic gases. Science 269:491–495. https://doi.org/10.1126/science.269.5223.491

Salameh T, Sauvage S, Afif C et al (2016) Source apportionment vs. emission inventories of non-methane hydrocarbons (NMHC) in an urban area of the Middle East: local and global perspectives. Atmos Chem Phys 16:3595–3607. https://doi.org/10.5194/acp-16-3595-2016

Shi J, Deng H, Bai Z et al (2015) Emission and profile characteristic of volatile organic compounds emitted from coke production, iron smelt, heating station and power plant in Liaoning Province. China Sci Total Environ 515:101–108. https://doi.org/10.1016/j.scitotenv.2015.02.034

Song M, Tan Q, Feng M et al (2018) Source Apportionment and Secondary Transformation of Atmospheric Nonmethane Hydrocarbons in Chengdu Southwest China. J Geophys Res Atmos 123:9741–9763. https://doi.org/10.1029/2018jd028479

Tang L, Qu J, Mi Z et al (2019) Substantial emission reductions from Chinese power plants after the introduction of ultra-low emissions standards Nature. Energy 4:929–938. https://doi.org/10.1038/s41560-019-0468-1

Venecek MA, Carter WPL, Kleeman MJ (2018) Updating the SAPRC Maximum Incremental Reactivity (MIR) scale for the United States from 1988 to 2010. J Air Waste Manag Assoc 68:1301–1316. https://doi.org/10.1080/10962247.2018.1498410

Wang P, Guo H, Hu J et al (2019) Responses of PM2.5 and O-3 concentrations to changes of meteorology and emissions in China. Sci Total Environ 662:297–306. https://doi.org/10.1016/j.scitotenv.2019.01.227

Wu W, Zhao B, Wang S et al (2017) Ozone and secondary organic aerosol formation potential from anthropogenic volatile organic compounds emissions in China. J Environ Sci 53:224–237. https://doi.org/10.1016/j.jes.2016.03.025

Wu X, Zhao L, Zhang Y et al (2015) Primary air pollutant emissions and future prediction of iron and steel industry in China. Aerosol Air Quality Res 15:1422–1432. https://doi.org/10.4209/aaqr.2015.01.0029

Xiong Y, Zhou J, Xing Z et al (2020) Optimization of a volatile organic compound control strategy in an oil industry center in Canada by evaluating ozone and secondary organic aerosol formation potential. Environ Res. https://doi.org/10.1016/j.envres.2020.110217

Yao Z, Shen X, Ye Y et al (2015a) On-road emission characteristics of VOCs from diesel trucks in Beijing, China. Atmos Environ 103:87–93. https://doi.org/10.1016/j.atmosenv.2014.12.028

Yao Z, Wu B, Shen X et al (2015b) On-road emission characteristics of VOCs from rural vehicles and their ozone formation potential in Beijing, China. Atmos Environ 105:91–96. https://doi.org/10.1016/j.atmosenv.2015.01.054

Zhang X, Gao S, Fu Q et al (2020) Impact of VOCs emission from iron and steel industry on regional O-3 and PM2.5 pollutions. Environ Sci Pollut Res 27:28853–28866. https://doi.org/10.1007/s11356-020-09218-w

Zheng H, Kong S, Xing X et al (2018) Monitoring of volatile organic compounds (VOCs) from an oil and gas station in northwest China for 1 year. Atmos Chem Phys 18:4567–4595. https://doi.org/10.5194/acp-18-4567-2018